

Registration Modeling and Simulation in Advanced Mix-and-Match Lithography

Warren W. Flack and Gary E. Flores

Ultratech Stepper, Inc., San Jose, CA 95134

Joseph C. Pellegrini

New Vision Systems, Watertown, MA 02172

Mark Merrill

KLA Instruments Corporation, San Jose, CA 95161

Registration models are well developed for environments using similar types of lithography equipment. In this arrangement, a 1:1 field size matching is the standard registration requirement. However, there is now significant interest in mix-and-match lithography utilizing systems with extremely large field sizes to increase wafer throughput on less critical process levels. This approach is widely accepted as a valuable technique to enhance cost of ownership for a manufacturing environment. In many cases, these large-field steppers have twice the field size of advanced reduction steppers. To properly characterize and optimize such a 2:1 matching scheme, it is necessary to consider the types of registration errors present and their sources.

A unique 2:1 field algorithm that appropriately accounts for the 2:1 field size matching has been developed. This model incorporates the grid model parameters for both lithography tools. A residual analysis is used to demonstrate the benefit of the new 2:1 field algorithm. Because of the complicated interactions of both the grid and intrafield component, application traditional of 1:1 registration models does not adequately minimize the mix-and-match overlay. For example, lens magnification on the wide field stepper can manifest itself as an apparent combination of scale

errors from both steppers plus a noncorrectable residual. The effects of such interactions are demonstrated through the use of a lithography overlay simulator for 2:1 field matching. Various scenarios provide insight into the impact of model parameters on the 2:1 field matching.

1. Introduction

Historically, the global competition in integrated circuit fabrication has been based on both technological and economic factors. However, fabrication costs are now becoming the single dominant issue as the price of new high-volume production facilities approaches the billion dollar level [1]. Since lithography equipment represents a large fraction of this investment cost, it is also an excellent area in which to pursue cost savings [1]. One technique that has been extremely successful in containing lithographic costs is mix-and-match lithography.

Mix-and-match lithography has been used to bridge different systems to derive the maximum benefits of each. In the early 1980s, mix-and-match was first used between scanners and steppers to take advantage of the installed base of scanners while achieving the resolution and overlay of the steppers for critical levels [2]. More recently, mix-and-match lithography has been used between steppers and extremely expensive, high-performance lithography equipment such as direct write-on wafer e-beam or x-ray systems [3]. This approach offered significant fabrication cost savings while maintaining technological advantages.

In general, a less costly and higher throughput lithography tool is used for the non-critical levels, while the higher resolution and more expensive lithography tool is only used on critical levels. This approach provides dramatic cost-of-ownership advantages over using the more expensive critical level lithography tool on all levels [1,4]. Higher throughput for non-critical levels can be achieved by systems with a large lens field size that reduces the number of exposure steps

required for each wafer. However, this larger field size must be an integer multiple of the field size of the second lithography tool to take advantage of the potential reduction in exposure steps. For example, the Ultratech 2244i 1x stepper has a rectangular field size of 22 x 44 mm, which is twice the 22 x 22 mm square field size of 5x reduction steppers from ASM, Canon and Nikon [5].

To obtain maximum performance when using multiple lithographic systems, each system must be calibrated or matched to the others [6]. Extensive analysis and modeling of overlay errors has been developed for the matching of similar systems. These overlay errors can be divided into intrafield and interfield systematic sources. The intrafield sources (dX and dY) model the overlay error sources within one field [7,8,9]:

$$dX(x,y) = T_{ix} + M_x x - \Theta_i y + \Psi_x xy + \Psi_y x^2 + D_3 x(x^2+y^2) + D_5 x(x^2+y^2)^2 \quad (1)$$

$$dY(x,y) = T_{iy} + M_y y + \Theta_i x + \Psi_y xy + \Psi_x y^2 + D_3 y(x^2+y^2) + D_5 y(x^2+y^2)^2 \quad (2)$$

where x and y are the coordinate location relative to the center of the field. For equations (1) and (2), the linear terms include die shift in x (T_{ix}) and y (T_{iy}), magnification in x (M_x) and y (M_y) and rotation (Θ_i). The nonlinear terms include trapezoid in x (Ψ_x) and y (Ψ_y) third order (D_3) and fifth order (D_5). The interfield sources (E_x and E_y) model the grid stage motion errors across the wafer [8,9]:

$$E_x(X,Y) = T_{gx} + S_x X - \Theta_g Y - \Phi Y \quad (3)$$

$$E_y(X,Y) = T_{gy} + S_y Y + \Theta_g X \quad (4)$$

where X and Y are the coordinate locations on the wafer. The interfield sources include translation error in X (T_{gx}) and Y (T_{gy}), wafer scaling magnification in X (S_x) and Y (S_y), wafer rotation (Θ_g), and wafer orthogonality (Φ).

These intrafield and interfield models assume identical field sizes, which implies 1:1 field matching. However, mix-and-match lithography frequently requires $n:1$ field matching for high throughput. To optimize such $n:1$ matching schemes, it is necessary to consider the types of registration errors present and their sources. This paper develops a grid overlay model for the 2:1 matching case and studies the interactions of grid and intrafield sources using a 2:1 lithography simulator.

2. Overlay Modeling

It is possible to have $n:1$ field matching when the field area on at least one stepper is n times as large as the field area on the other steppers. The specific overlay model developed in this paper will be for 2:1 grid matching, but it can be extended to the general $n:1$ case. This analysis will refer to the Ultratech 2244i and generic large field systems as a wide field stepper, or w in equation subscripts. The 5x reduction steppers and similar systems will be referred to as narrow field steppers, or n in equation subscripts. Note that the following analysis is independent of the magnification reduction ratio of either the wide field or the narrow field systems.

The mix-and-match case to be modeled assumes the base layer is blind stepped onto the wafer using a narrow field stepper. The second level is then patterned by a wide field stepper using alignment targets placed on the base level. For each stepped position, the wide field stepper simultaneously patterns two horizontally spaced narrow stepper fields as shown in Figure 1. Here ΔX and ΔY represent the stage motion in the X and Y directions respectively. To simplify the following numerical analysis, the pattern of measured overlay structures should be symmetric across the X and Y axes in both the narrow field and wide field coordinate systems.

The total grid stage motion errors for both steppers can be obtained from Equations (3) and (4):

$$V_{xtotal}(X_n, Y_n, X_w, Y_w) = T_{gxn} + S_{xn}X_n + \Theta_{gn}Y_n - \Phi_n Y_n + T_{gxw} + S_{xw}X_w + \Theta_{gw}Y_w - \Phi_w Y_w \quad (5)$$

$$V_{ytotal}(X_n, Y_n, X_w, Y_w) = T_{gyn} + S_{yn}Y_n + \Theta_{gn}X_n + T_{gyw} + S_{yw}Y_w + \Theta_{gw}X_w \quad (6)$$

The grid error terms described above are not necessarily actual, but rather are apparent or effective errors. Therefore, the variables can be redefined in terms of separable or inseparable type coefficients. Inseparable coefficients describe errors that are fully correctable by application at either stepper and include x translation (T_x^*), y translation (T_y^*), y scale (S_y^*) and orthogonality (Φ^*). Combinations of stepper effects for this type of component are additive. However, separable components require independent corrective action on both steppers to minimize overlay error. This occurs since intrafield errors are coupled to the grid errors in these equations, and is the fundamental motivation for the development of this 2:1 grid model.

The total errors in Equations (5) and (6) can be transformed into a single coordinate system. The narrow field errors are translated to the wide field coordinate system using the geometric relationship in Figure 1. The inseparable coefficients are then substituted into the transformed equations to yield:

$$V^*x(X_n, Y_n, X_w, Y_w) = T_x^* + S_{xn}X_n + \Theta_{gn}Y_n - \Phi^*Y_n + S_{xw}X_w + \Theta_{gw}Y_w \quad (7)$$

$$V^*y(X_n, Y_n, X_w, Y_w) = T_y^* + S_y^*Y_n - \Theta_{gn}X_n - \Theta_{gw}X_w \quad (8)$$

This technique is tantamount to solving for grid corrections in the wide field stepper coordinate system. Here the equations are actually under determined because of the inseparable grid terms.

The coefficients in Equations (7) and (8) can be determined by creating a system of equations that can be solved by least squares techniques using actual overlay data $M_x(X,Y)$ and $M_y(X,Y)$ [10].

The 2:1 model results obtained are subtracted from the overlay data to create the residual arrays

$R_x^*(X,Y)$ and $R_y^*(X,Y)$. This is the difference between the measured data points and the estimate of the overlay error at that point:

$$R_x^*(X,Y) = M_x(X,Y) - V^*_x(X,Y) \quad (9)$$

$$R_y^*(X,Y) = M_y(X,Y) - V^*_y(X,Y) \quad (10)$$

If additional assumptions are made about the pattern of overlay measurements, it is possible to combine intrafield terms into the grid algorithm. This scenario will be analyzed fully in future work.

3.0 Experimental Verification

The validity of the 2:1 model was determined experimentally using an Ultratech Stepper Model 2244i as the wide field stepper and a Canon Model FPA 2500i2 as the narrow field stepper. The Ultratech Stepper Model 2244i is designed for i-line lithography with a field size of 22 x 44 field size [5]. Also incorporating i-line optics, the Canon Model FPA 2500i2 stepper provides a field size of 22 x 22 mm square. Thus, two fields from the narrow field stepper can be positioned within a single 22 x 44 mm field on the Ultratech 2244i. Using this set-up, wafers from the backend segment of a submicron CMOS process were evaluated. Overlay was measured on a KLA 5700 Coherence Probe Microscope using 66 box-in-frame structures spread across the Ultratech field. A total of 14 Ultratech fields were measured on nine 8-inch wafers for a total of 924 overlay measurements per wafer. The details of the experimental methodology and metrology are fully described elsewhere [10].

Three different grid models were studied using this data set. These models included the 2:1 model algorithm developed in this paper, a 1:1 model with the narrow field stepper as the reference level, and a 1:1 model with the wide field stepper as the reference level. The 2:1 model grid coefficients

were calculated using a beta site version of Mono-Lith[®] containing the new algorithm[9], while model coefficients for the 1:1 models were determined from KLASS III[®] software[11]. Experimental results comparing the models illustrate the superior performance of the 2:1 algorithm. Both 1:1 models show comparable residuals while the 2:1 model shows a 29% improvement [10]. These results experimentally establish the advantages of the 2:1 model.

4. Simulation Results

4.1 Simulation Modeling

Simulation of grid and intrafield errors for 2:1 field matching provides an illustrative technique to understand the resulting overlay error. A simulator designed specifically for 2:1 field matching was developed for this project using Mono-lith[®] software. The 2:1 simulator allows generation of grid and intrafield errors for narrow and wide field steppers using Equations (1) through (4).

The simulated results consist of a 4 by 4 wafer matrix of narrow fields, each with a field size of 22 x 22 mm. Alternatively, this can be viewed as a wide field matrix of 2 columns and 4 rows with a field size of 44 x 22 mm. The intrafield grid consists of 9 locations in a 3 by 3 array for the narrow field stepper, where each grid location is spaced 6.5 mm. For the wide field stepper the same 6.5 mm spacing was used for a total of 18 grid locations in an array of 3 rows and 6 columns. Thus, this format provides for a total of 144 grid locations for visual representation.

To understand the simulation overlay errors for 2:1 field matching, it is effective to examine the error sources for the narrow and wide field steppers independently and then show the net effect of both for mix-and-match. Because of the 2:1 matching geometry in the x axis, comparable error sources from both the wide field and narrow field steppers will not necessarily provide zero

residual error. The four scenarios examined are wafer scale magnification in X , intrafield magnification, wafer grid orthogonality and intrafield rotation.

4.2 Wafer Scaling Magnification in X

Figure 2 illustrates the simulation of wafer scaling magnification in X (S_x) with errors of +10 ppm (parts per million) for the narrow field stepper and -5 ppm for the wide field stepper. The figure shows the narrow field errors, the wide field errors and the combination errors in the top, center and bottom portions respectively. The effect of the +10 ppm X wafer scale for the narrow field results in a stepped increase in overlay error in the X direction for each field from the center. In comparison, the -5 ppm wide field scale error results in an incremental error in the opposite direction from the narrow field scale error in the X direction, but the errors remain consistent over the wide field geometry. The combination of the X scale errors for mix-and-match results in a net residual scale error. It is interesting that the combined error is zero for the center two columns of the narrow field, while the outer two rows have a net residual error. Clearly, this type of net error would be impossible to explain in a n:1 field model.

4.3 Intrafield Magnification in x (M_x) and y (M_y)

The next example considers equal and opposite intrafield magnification errors on both steppers. Figure 3 shows the intrafield magnification in x (M_x) and y (M_y) for the narrow field and wide field steppers of +10 ppm and -10 ppm respectively. For the narrow field stepper, the intrafield magnification of +10 ppm results in maximum error vector of 220 nm at the edge of the field (10 ppm times the field size of 22 mm) in both the x and y directions. For the wide field stepper an intrafield magnification -10 ppm results in a maximum error vector of 220 ppm in the y dimension at the edge of the field, but in the opposite direction. However, the error vector is 440 nm in the x

direction since the wide field dimension is twice that of the narrow field. Therefore, when both the narrow and wide field magnification errors are combined the net result is a residual x mean offset difference between alternating narrow field columns. This net residual can be viewed within the wide field domain as a symmetric x mean offset across the left and right portions of the field that are equal but of opposite magnitude.

4.4 Wafer Grid Orthogonality

Wafer grid orthogonality (Φ) is another interesting example where it is useful to consider equal and opposite errors on the narrow and wide field steppers. Here grid orthogonality errors of -10 ppm and +10 ppm for the narrow field and wide field steppers are shown in the top and center portions of Figure 4. Since wafer grid orthogonality occurs as a step change in wafer field step location, all vector errors are oriented in the same x and y direction for a given wide or narrow field position. Further, since orthogonality is a function of the wafer grid, so the error magnitude is dependent on grid location. It is interesting to evaluate the impact of combining the narrow and wide field grid components. In this case two horizontal narrow fields containing two different error vector magnitudes are combined with a single wide field containing constant error vectors over the entire field. The net result is a mean y offset error across the wide field. These errors occur in alternating narrow field columns with equal and opposite errors. Here the x component of the individual orthogonality errors combine for a net zero offset. What is also unique is that the grid based nature of the orthogonality error no longer exists. Again, such results can not be explained by a classical 1:1 field model.

4.5 Intrafield Rotation

Intrafield rotation (Θ_1) due to reticle placement errors also shows a similar behavior to that of the wafer grid orthogonality. In this example intrafield rotation errors of -10 ppm and +10 ppm for the narrow field and wide field steppers are shown in the top and middle portions of Figure 5. In both cases, the intrafield rotation point is at the x and y center of each stepper field. However, unlike the orthogonality example, intrafield rotation does not depend on field placement. The combined effect of these errors is shown in the bottom portion of Figure 5. Here, the residual error is a y mean offset across the wide field stepper domain. As in the last example, these errors occur in alternating narrow field columns with equal and opposite magnitude.

5. Conclusions

With the continued escalating costs of advanced lithography equipment for the semiconductor industry, mix-and-match lithography is becoming widely accepted as a necessary cost containment measure. However, the lithography inherent to mix-and-match requires $n:1$ field matching which can not be optimized fully using classic $1:1$ models.

A unique $2:1$ grid algorithm and simulator have been developed for this application. The $2:1$ grid algorithm, which applies corrective action on both the narrow and wide field steppers, has been experimentally shown to provide significant improvement over the classical approach of corrective action on either stepper individually. Simulation of error sources for $2:1$ field matching has also been explored to understand the unique effects of registration error sources resulting from the $2:1$ geometry. For example, lens magnification on either the wide field or narrow field stepper can manifest itself as apparent combinations of mean scale errors from both steppers. It is also possible to have intrafield errors or mean offset differences between alternating pairs of narrow stepper fields and within the wide stepper fields due to equal and opposite errors such as

orthogonality, intrafield rotation and intrafield magnification. These effects illustrate the necessity of using proper models and overlay sampling schemes for characterizing and optimizing overlay errors in any n:1 matching domain.

6. References

1. J. Maltabes, M. Hakey, A. Levine, *SPIE Optical/Laser Lithography VI Proc.* **1927**, (1993).
2. W. Arnold., *SPIE Optical Microlithography II Proc.* **394**, 87 (1983).
3. W. Flack, D. Dameron, G. Maleck and V. Alameda, *SPIE Electron-Beam, X-Ray and Ion Beam Submicrometer Lithographies for Manufacturing II Proc.* **1674**, 450 (1992).
4. M. Perkins and J. Stamp, *SPIE Optical/Laser Microlithography V Proc.* **1674**, 559 (1992).
5. G. Flores, W. Flack, L. Dwyer, *SPIE Optical/Laser Lithography VI Proc.* **1927**, 899 (1993).
6. A. Yost and W. Wu, *SPIE Integrated Circuit Metrology, Inspection and Process Control III Proc.* **1087**, 233 (1989).
7. J. Armitage, *SPIE Integrated Circuit Metrology, Inspection and Process Control II Proc.* **921**, 207 (1988).
8. M. van den Brink, C. de Mol and R. George, *SPIE Integrated Circuit Metrology, Inspection and Process Control II Proc.* **921**, 3 (1988).
9. Mono-Lith[®] Reference Manual, version 2.08, Registration Models and Algorithms, pp. 315.
10. W. Flack, G. Flores, J. Pellegrini and M. Merrill, *SPIE Optical/Laser Microlithography VII Proc.* **2197**, (1994).
11. KLASS III[®] Reference Manual, Appendix Models and Algorithms.

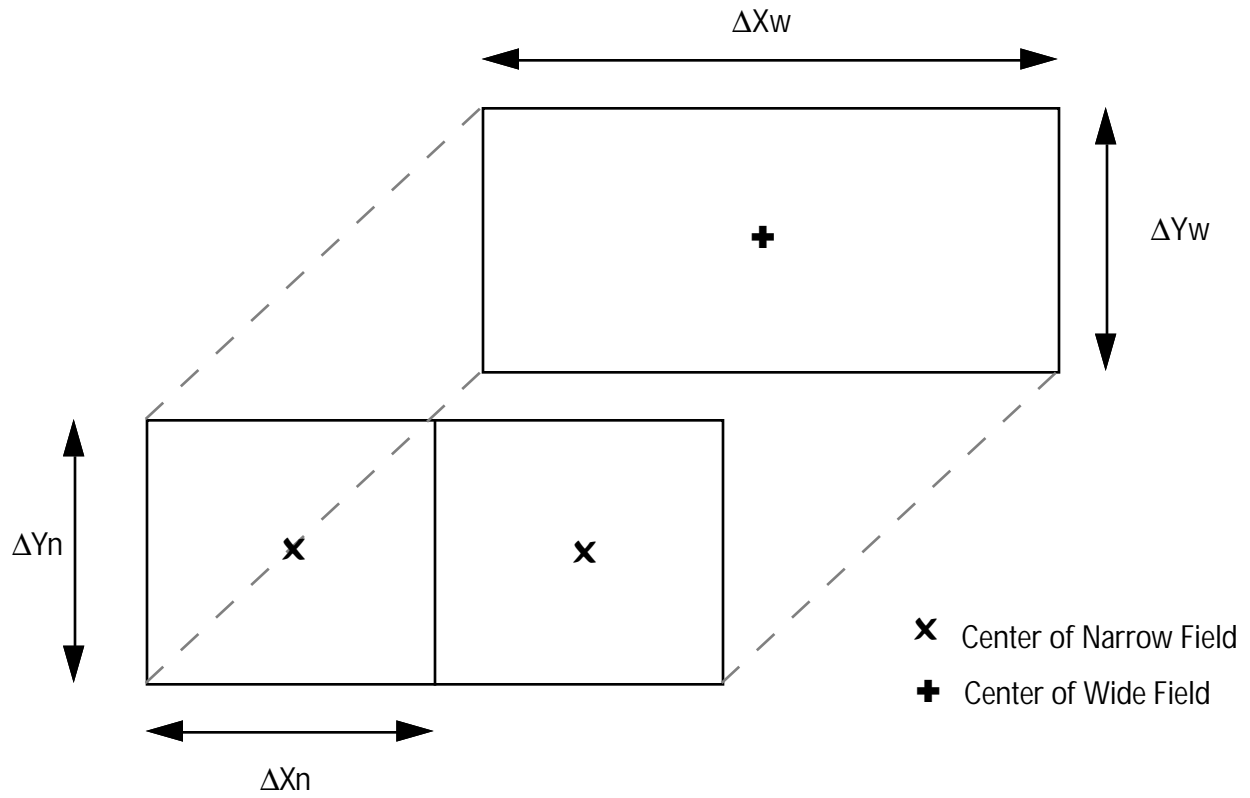


Figure 1: Exploded view of 2:1 field overlay

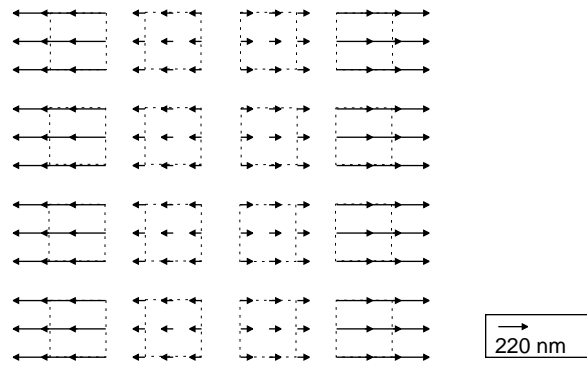
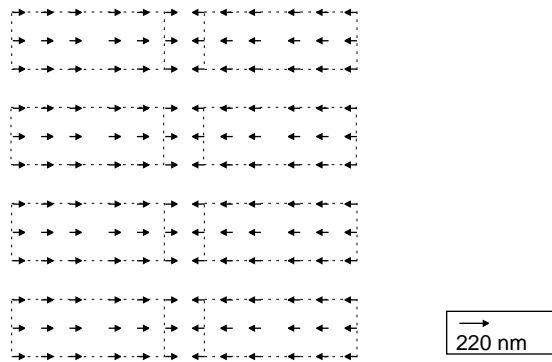
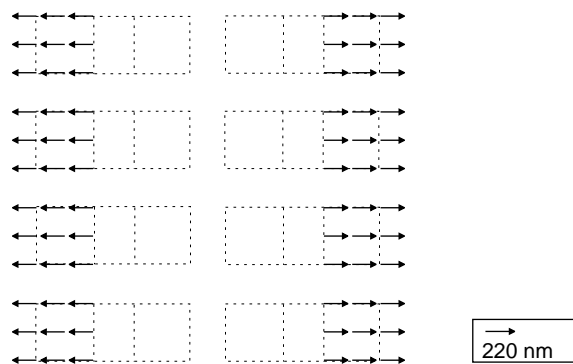
*Narrow Field**Wide Field**Combination*

Figure 2: Simulation of X scale errors on the wafer grid. The narrow field error is +10 ppm and the wide field error is -5 ppm.

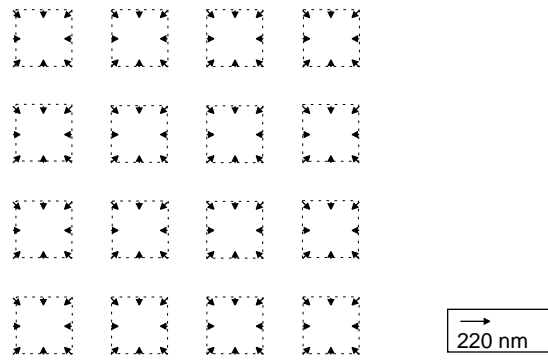
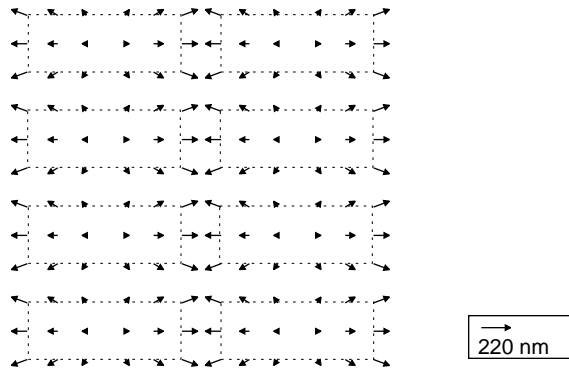
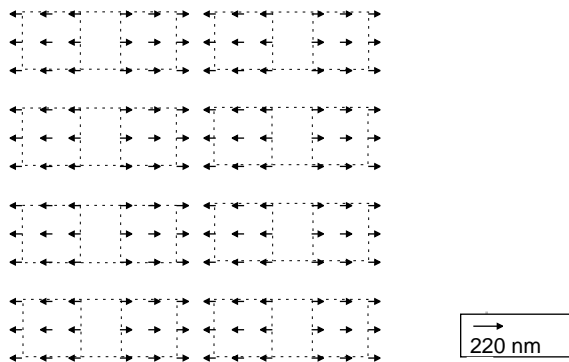
*Narrow Field**Wide Field**Combination*

Figure 3: Simulation of intrafield magnification errors. The narrow field error is 10 ppm and the wide field error is -10 ppm.

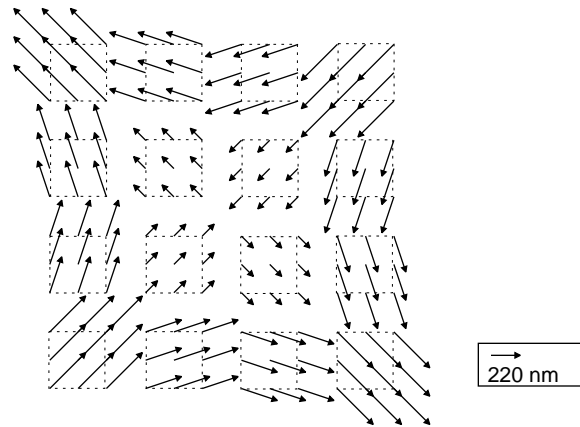
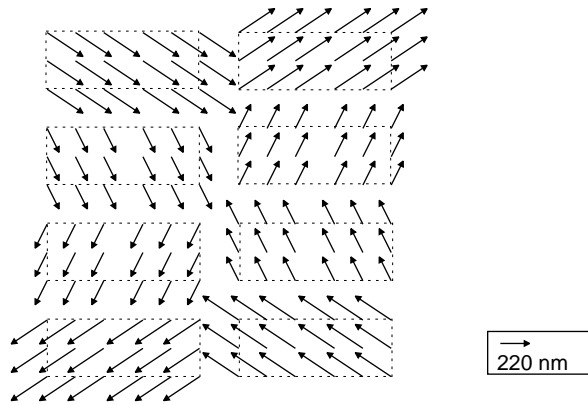
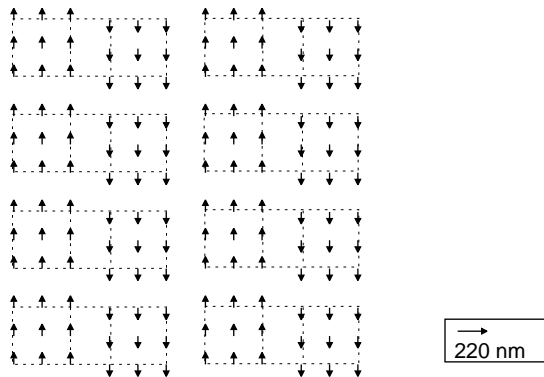
*Narrow Field**Wide Field**Combination*

Figure 4: Simulation of orthogonality on the wafer grid. The narrow field error is -10 ppm and the wide field is +10 ppm.

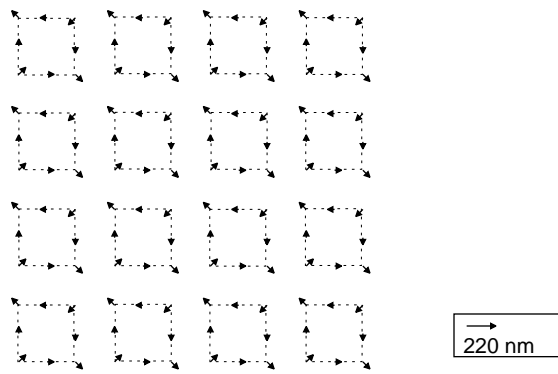
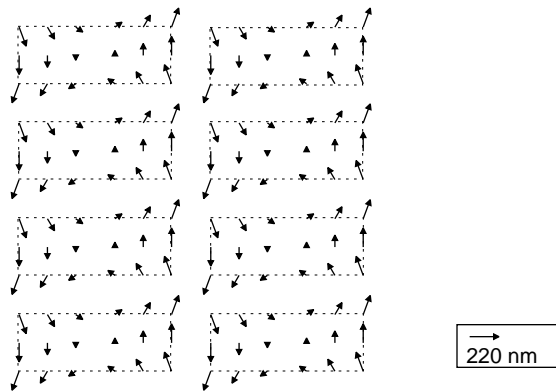
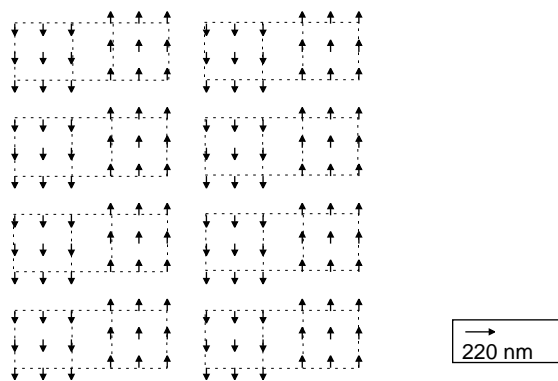
*Narrow Field**Wide Field**Combination*

Figure 5: Simulation of intrafield rotation errors. The narrow field error is -10 ppm and the wide field error is +10 ppm.